In Vivo Probe Measurement Technique for Determining Dielectric Properties at VHF Through Microwave Frequencies

EVERETTE C. BURDETTE, MEMBER, IEEE, FRED L. CAIN, MEMBER, IEEE, AND JOSEPH SEALS, MEMBER, IEEE

Abstract—**A novel probe technique for the determination of dielectric properties of semisolid materials and living tissues *in situ* is described experimentally and theoretically. This method, based on an antenna modeling theorem, offers unique advantages over conventional dielectric measurement techniques including 1) an ability to perform living (*in vivo*) tissue dielectric measurements, 2) elimination of the need for tedious sample preparation, 3) the ability to obtain continuous dielectric property data from below 0.1 GHz to above 10 GHz, and 4) the ability to process data on a real time basis. Results of system performance evaluation via measurements of standard liquid dielectric and *in vivo* tissue data are presented.**

I. Introduction

IT IS WELL recognized that the dielectric properties of a biological system determine the coupling and absorption of nonionizing electromagnetic (EM) energy into that system. Therefore, a prior knowledge of the dielectric properties of the biological system of interest is essential either to effectively employ EM radiation in beneficial biomedical applications or to adequately determine safe levels for personnel exposure to EM radiation. In view of these facts, it may be concluded that a measurement system capable of adequately determining the living (*in vivo*) dielectric properties of biological tissues would play a significant role in any well-founded effort involving tissue/EM energy interactions.

Areas of biomedical research which would benefit from accurate dielectric property information include beneficial applications such as EM-induced hyperthermia for cancer treatment, EM thawing of cryogenically preserved tissue and organs, and diathermy applications [1]–[4]. Tissue dielectric property information is also potentially useful in investigations of physiological processes such as organ activity or inactivity, induced physiological changes, diseases, etc., that would affect various tissue components, and hence, the tissue dielectric properties. Once dielectric property changes have been correlated with physiological changes, this information would be useful as a measurement/diagnostic indicator of these changes.

Dielectric property information is also essential to the determination of EM radiation hazards with respect to personnel [5]. The level of electromagnetic energy which is considered to be below the level which constitutes a potential hazard to personnel working in that environment is dependent upon many factors. One of these factors is the interaction of the incident EM field with various tissues and organ systems, which is in turn dependent upon the local geometry and the dielectric properties of those systems. Therefore, an accurate knowledge of the *in vivo* dielectric properties of the principal tissues and organs in the body is crucial to the accurate determination of absorbed power and its spatial distribution. Without accurate knowledge of the dielectric properties, any computation of power absorption from known or measured fields is at best an estimate.

A variety of conventional measurement techniques can be utilized to measure the dielectric properties of biological tissues [6]. However, the majority of these techniques have several limitations. For example, tissue excision is often required, which makes measurement of the *in vivo* dielectric properties of the tissue impossible [7]. This is a significant problem since factors such as temperature, blood flow, and possibly physiological differences between living and nonliving tissue influence the tissue's dielectric properties. Also, once the tissue sample is excised, it must be carefully prepared to conform to the exact dimensions of a special sample holder. Since precise tissue sample preparation is usually extremely difficult, improperly prepared samples are often a major source of measurement error. Another shortcoming of conventional measurement techniques is their limited frequency range of operation. This makes it necessary to implement several different measurement systems in order to obtain data over any appreciable frequency range.

The problems associated with conventional dielectric property measurement techniques have been overcome by the recent development of a truly *in vivo* probe measurement technique [8]–[12]. The measurement concept used to develop this new technique is based on the use of an antenna modeling theorem and on the application of more precise, microprocessor-controlled, microwave measurement instrumentation. The theorem relates the change in free-space terminal impedance of an antenna when inserted into a material to the dielectric and magnetic properties of that material [13]. A short monopole antenna, suitable for insertion into living tissues, is used as the *in vivo* probe since its terminal impedance is easily

Manuscript received May 31, 1979; revised November 2, 1979. This work was supported by ARO under Grant DAAG29-75-G-0182.

The authors are with Biomedical Research Branch, Electronic Technology Laboratory, Engineering Experiment Station, Georgia Institute of Technology, Atlanta, Georgia 30332.

0018-9480/80/0400-0414$00.75 ©1980 IEEE

described analytically [14]. A Hewlett-Packard network analyzer used in conjunction with error-correction routines and a semiautomated data acquisition/data processing system permits the accurate determination of the required electrical characteristics of the *in vivo* probe and tissue being measured.

Described herein is a simple, flexible, and accurate method for determining the dielectric properties of *in vivo* tissues as well as liquid and semisolid materials over a wide frequency range extended from the low VHF region well into the microwave (10-GHz) region of the frequency spectrum. The efforts expending in the development of this technique have involved both the analysis and the development of a suitable probe and associated instrumentation for performing *in vivo* dielectric measurements over this broad frequency range. Specific areas of investigation included 1) probe analysis, design, and fabrication, 2) system development, 3) systemic error correction techniques, 4) determination of probe measurement accuracy, and 5) determination of the *in vivo* dielectric properties of various tissues which included muscle, kidney, fat, brain, and blood.

II. Theoretical Basis

The theoretical basis of the *in vivo* measurement probe stems from the application of an antenna modeling theorem to the characterization of unknown dielectric media [12]–[15]. In a nonmagnetic medium where $\mu = \mu_0$, the antenna modeling theorem can be expressed mathematically as

$$\frac{Z(\omega, \epsilon^*)}{\eta} = \frac{Z(n\omega, \epsilon_0)}{\eta_0} \tag{1}$$

where

$\omega = 2\pi f$	angular frequency (radians),
$\eta = \sqrt{\mu_0/\epsilon^*}$	the complex intrinsic impedance of the dielectric medium,
$\epsilon^* = \epsilon' - j\epsilon''$	the complex permittivity of the dielectric medium,
$\eta_0 = \sqrt{\mu_0/\epsilon_0}$	the intrinsic impedance of free space,
ϵ_0	the permittivity of free space,
$n = \sqrt{\epsilon^*/\epsilon_0}$	the complex index of refraction of the dielectric medium relative to that of air.

This theorem is applicable for any probe provided an analytical expression for the terminal impedance of the antenna is known both in free space and in the dielectric medium under study. The theorem as stated in (1) assumes that the medium surrounding the antenna is infinite in extent, or conversely, the theorem is valid as long as the probe's radiation field is contained completely within the medium.

When the length of the probe antenna is approximately one-tenth wavelength or greater, a radiation field exists. In cases where the penetration depth in the medium under study is greater than the sample volume, errors are introduced in the measurement of the complex impedance of the medium because the field is not contained within the sample. The extent of the error introduced in the measurement of the antenna terminal impedance can be expressed quantitatively by use of the reaction theorem [16]. The impedance Z_v of a short antenna in a nonmagnetic medium of volume V can be written in terms of the impedance Z of the antenna in free space and the permittivity of the lossy volume as

$$Z_v = Z - \frac{j\omega}{I^2} \int_V (\epsilon - \epsilon_0) \bar{E}' \cdot \bar{E}\, dV \tag{2}$$

where I is the current in the antenna, $\bar{E}'$ is the electric field in lossy volume, and $\bar{E}$ is the electric field in free space.

The difference between the antenna impedance in an infinite volume (Z_{inf}) and a finite volume (Z_v) is

$$\Delta Z = Z_V - Z_{\text{inf}} = \frac{j\omega}{I^2} \int_{(\text{all space } V)} (\epsilon - \epsilon_0) \bar{E}' \cdot \bar{E}\, dV. \tag{3}$$

The ratio $\Delta Z/Z$ gives the error in calculation of the probe impedance Z_V in a finite volume, when an infinite volume is assumed. For low-loss samples, ΔZ can be considerable, but for samples having high loss, such as biological tissue, it is possible to define a volume which approximates the infinite volume required.

For short monopole probes whose center conductor approaches zero length, no appreciable radiated field exists, but the probe's fringing field is present. Thus for very short (or infinitesimal) probes whose length approaches zero, the minimum sample volume required for accurate measurements is primarily dependent upon the distance between the tightly coupled center and outer conductors of the probe. For example, measurement results which are in good agreement with published dielectric property data, have been obtained using sample volumes as small as 0.008 in^3 (0.13 cm^3).

A. Short Monopole Probe

The terminal impedance of a short monopole antenna ($\lambda/10$ or less in length) in free space is given by

$$Z(\omega, \epsilon_0) = A\omega^2 + \frac{1}{jC\omega} \tag{4}$$

where A and C are constants determined by the physical dimensions of the antenna [14]. From a knowledge of the antenna constants (A and C) and the magnitude and phase of the complex impedance $Z(\omega, \epsilon^*)$ of the antenna in a lossy medium, the values of relative dielectric constant, conductivity, and loss tangent can be obtained from (1) as follows. The complex permittivity can be represented in terms of the relative dielectric constant and loss tangent of the medium as

$$\epsilon^* = \epsilon_0(K' - jK'') = K'\epsilon_0(1 - j\tan\delta) \tag{5}$$

where $K' = \epsilon'/\epsilon_0$ is the relative dielectric constant, $K'' = \epsilon''/\epsilon_0$ is the relative loss factor, and $\tan\delta = \sigma/\omega\epsilon'$.

The impedance relation in (1) can now be written in the

form:

$$Z(\omega,\epsilon^*)=\sqrt{\frac{\epsilon_0}{\epsilon^*}}\ Z\left(\frac{\epsilon^*}{\epsilon_0}\omega,\epsilon_0\right) \tag{6}$$

where $n=\sqrt{\epsilon^*/\epsilon_0}$.

Utilizing the form of antenna impedance given in (4), one obtains

$$Z(\omega,\epsilon^*)=A\omega^2\sqrt{\frac{\epsilon^*}{\epsilon_0}}+\frac{1}{jC\omega\left(\frac{\epsilon^*}{\epsilon_0}\right)}. \tag{7}$$

Equation (7) relates the complete impedance of a lossy dielectric medium at a frequency ω to the relative complex dielectric constant of the medium. In terms of dielectric constant and loss tangent, (7) becomes

$$Z(\omega,\epsilon^*)=A\omega^2\sqrt{K'(1-j\tan\delta)}+\frac{1}{jC\omega[K'(1-j\tan\delta)]} \tag{8}$$

which is a restatement of the theorem in (1) for a short monopole. This equation can be placed in the form $Z=R+jX$ which reduces to two real equations to give

$$R=\frac{\sin 2\delta}{2K'\omega C}+A\sqrt{K'}\,\omega^2\sqrt{\frac{\sec\delta+1}{2}} \tag{9}$$

and

$$X=\frac{\cos^2\delta}{K'\omega C}+A\sqrt{K'}\,\omega^2\sqrt{\frac{\sec\delta-1}{2}}\ . \tag{10}$$

The parameters R and X are the real and imaginary components of the measured impedance, A and C are the physical constants of the probe, and all other parameters are known except K' and δ. Because the inverse pair of equations corresponding to (9) and (10) cannot be easily obtained, an iterative method of solution is utilized. The second term in both (9) and (10) is small at low frequencies. Neglecting these high-frequency terms, one obtains the equations:

$$R=\frac{\sin 2\delta}{2K'\omega C} \tag{11}$$

and

$$X=\frac{\cos^2\delta}{K'\omega C}. \tag{12}$$

The solutions of these equations are easily obtained by noting that $\tan\delta=R/X$.

The values of K' and δ obtained above can be used to solve (9) and (10) by iteration. Letting $K'=u^2$, (9) and (10) are expressed as

$$\left[A\omega^2\sqrt{\frac{\sec\delta+1}{2}}\right]u^3-Ru^3+\frac{\sin 2\delta}{2\omega C}=0 \tag{13}$$

and

$$\left[A\omega^2\sqrt{\frac{\sec\delta-1}{2}}\right]u^3-Xu^2+\frac{\cos^2\delta}{\omega C}=0. \tag{14}$$

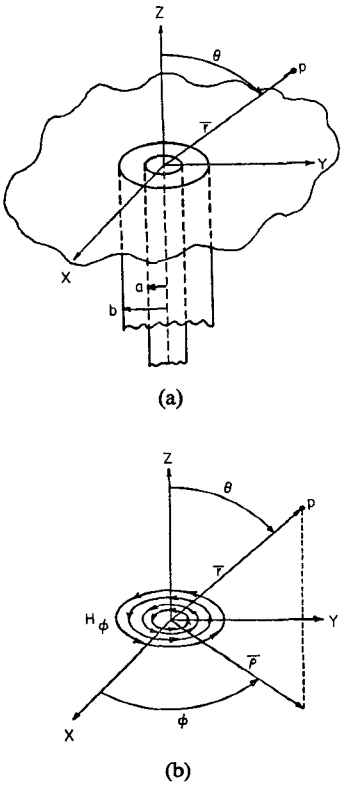

Fig. 1. Coaxial transmission line opening onto a ground plane. (a) Physical problem. (b) Equivalent EM problem.

Utilizing the low-frequency solution of δ obtained from (11) and (12), (13) can be solved for u, and hence K'. The correct values of δ and K' will satisfy both (13) and (14) exactly. This fact allows an iteration about both the low-frequency values until a K' is determined by (13) which exactly satisfies (14). This pair of K' and δ is the desired solution of (9) and (10), where K' is the relative dielectric constant and $\tan\delta$ is the loss tangent of the material.

B. Infinitesimal Probe

For the case of an infinitesimal coaxial probe where the extended length of the center conductor approaches zero, the impedance is totally reactive in free space. In that case, the probe is essentially an open-circuit transmission line which may be represented by a coaxial line opening onto a ground plane, as illustrated in Fig. 1. The radial electric field E_ρ over the aperture is the transmission-line mode of the coax and is given by

$$E_\rho=\frac{-V}{\rho\log(b/a)} \tag{15}$$

where V is the voltage between the inner and outer conductors at the open end. Applying the equivalence principle [17], E_ρ can be replaced by a magnetic current sheet $H_\phi=-E_\rho$. This magnetic current sheet acts as an electric dipole having an electrical vector potential in the ϕ direction. For this case, it is shown by Harrington [17] that the radiation field is given by

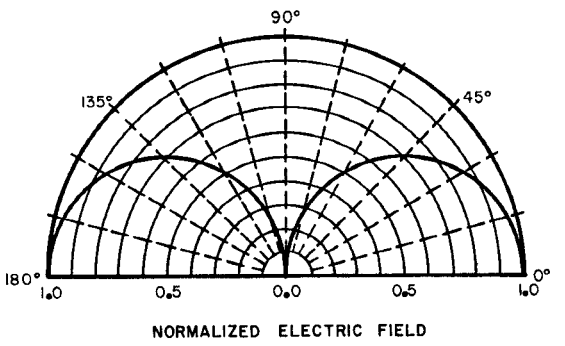

Fig. 2. Normalized free-space radiation field pattern of a coaxial transmission line opening onto a ground plane plotted as a function of polar angle.

$$H_\phi = \frac{\omega\epsilon\pi V(b^2-a^2)}{2\lambda r\log(b/a)}\, e^{-jkr}\sin\theta \tag{16}$$

where $k=2\pi/\lambda$ is the wavenumber, λ is the wavelength, and $E_\theta=\eta H_\phi$. The radiation field pattern of a coaxial transmission line opening into a ground plane is shown in Fig. 2, and the power radiated P_r, from the end of the coaxial line is given by

$$P_r = \frac{4\pi V^2}{3\eta}\left|\frac{\pi^2(b^2-a^2)}{\lambda^2\log(b/a)}\right|^2 \tag{17}$$

where the symbols are as defined previously and $\pi(b^2-a^2)$ is the area of the opening between the inner and outer conductors. Equation (17) illustrates that the power radiated varies inversely as λ^4 and that for a small-diameter coaxial line whose impedance is 50 Ω, the quantity within the absolute value symbols approaches zero.

An alternate examination of the radiated power of the infinitesimal monopole probe yields a result which agrees with the results obtained for treatment of the problem as a coaxially fed aperture, as given by (17). The radiation resistance R_r of the monopole is a function of the height of the monopole above the ground plane, or in this case, the length of the center conductor of the probe [14], [18]. As the extended length of the probe approaches zero, $R_r\to 0$ and no power ($P_r=I^2R_r$) is radiated. By expressing the terminal impedance of the probe in the form:

$$Z = R_r - jX \tag{18}$$

it can be seen that as $R_r\to 0$, the probe impedance becomes

$$Z = -jX \tag{19}$$

where Z is totally reactive (X is the reactance).

The infinitesimal monopole probe behaves like an open-circuited coaxial line which has been previously analyzed [14], [17], [19]. The impedance of an open-circuited line in free space is

$$Z(\omega,\epsilon_0) = \frac{1}{j\omega C} \tag{20}$$

where C is as defined in (4). When the probe is inserted into a lossy dielectric medium, (20) becomes

$$Z(\omega,\epsilon^*) = \frac{1}{j\omega\epsilon^* C} \tag{21}$$

where the symbols are as defined previously. Expanding the impedance expression of (20) in the antenna modeling theorem yields

$$Z(\omega,\epsilon^*) = \frac{1}{j\omega C[K'(1-j\tan\delta)]}. \tag{22}$$

This same expression is obtained by substituting the complex permittivity, ϵ^*, and probe capacitance expression (in free space) for ϵ^*C in (21). Therefore, for the case of an open-circuit transmission line, the final probe antenna impedance resulting from the antenna modeling theorem (8) reduces to the expression given by (22).

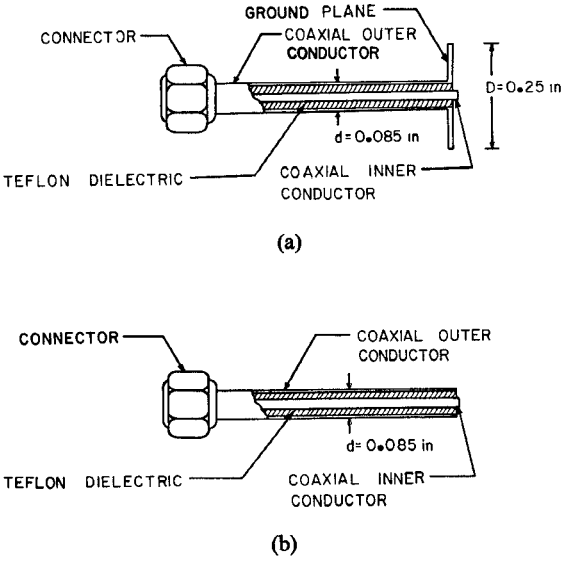

Fig. 3. Two configurations of the infinitesimal probe. (a) Probe with ground plane. (b) Probe without ground plane.

III. Probe Measurement System

A. Probe Configurations

A number of probe configurations have been investigated. The lengths of the extended center conductor of the probes have ranged from infinitesimal lengths of less than 0.02 in in length to lengths of 0.4 in, and probe outside diameters have ranged from the size of a #18 hypodermic needle (approximately 0.042 in) to 0.141 in. Although several infinitesimal monopole measurement probes have been fabricated from 0.085-in diameter semirigid coaxial cable, the two basic probe configurations which have been used most extensively are schematically illustrated in Fig. 3.

The *in vivo* measurement probes (Fig. 3) are each fabricated from a section of open-ended semirigid coaxial cable with a slightly extended center conductor. The small circular ground plane, shown in Fig. 3(a), minimizes fring-

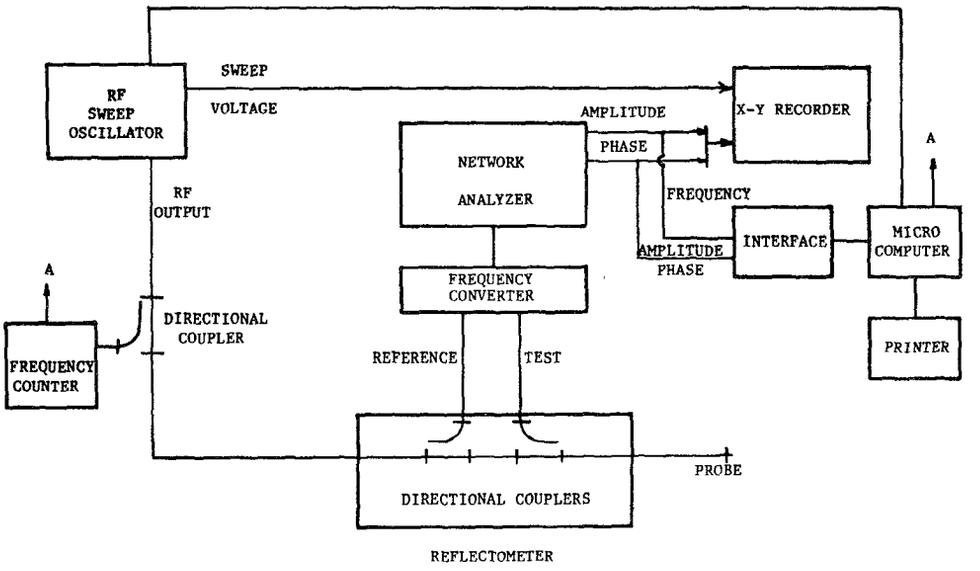

Fig. 4. Block diagram of *in vivo* dielectric property measurement system consisting of probe, network analyzer, and associated instrumentation.

ing effects. An SMA connector is attached to the probe by first removing the center conductor and teflon dielectric material. The connector is then soldered to the outer conductor followed by reassembly of the probe using the center conductor as the center pin of the connector, thus avoiding additional soldering. In this manner, it is possible to attach the SMA connector without heating the teflon dielectric. While disassembled, the center and outer conductors of the probe are first flashed with nickel plating and then gold plated. Plating the probe with an inert metal, such as gold, greatly reduces chemical reactions between the probe and the electrolyte in the tissue. This process virtually eliminates oxidation of the probe's metallic surfaces and helps to minimize electrode polarization effects at lower frequencies (0.01–0.1 GHz).

B. Probe Measurement System

The impedance measurement instrumentation employed to measure the terminal impedance of the probe is schematically illustrated in Fig. 4. The key components of the measurement system are the probe and the network analyzer, which is a Hewlett-Packard Model 8410B. The relative amplitude and phase difference between the reference and reflected signal channels is measured by the network analyzer, which functions as an amplitude and phase comparator. The network analyzer yields the terminal impedance of the probe in terms of the magnitude and phase angle of the reflection coefficient, and these data are used as input data to a computer algorithm which corrects systemic measurement errors and computes the dielectric property information. A semiautomated data acquisition/data processing system whose key components are an analog/digital converter and microprocessor was also designed and implemented to increase the rate at which *in vivo* dielectric data could be acquired and processed.

C. Microwave Measurement Error Correction and Calibration

When the network analyzer system is used for performing microwave measurements, there exist certain inherent measurement errors which can be separated into two categories: instrument errors and test set/connection errors [20]. Instrument errors are measurement variations due to noise, imperfect conversions in such equipment as the frequency converter, crosstalk, inaccurate logarithmic conversion, nonlinearity in displays, and overall drift of the system. Test set/connection errors are due to the directional couplers in the reflectometer, imperfect cables, and the use of connector adapters. The instrument errors exhibited by the HP 8410B Network Analyzer are very small. Noise is specified to be less than -78 dBm equivalent input noise, and the isolation between channels is greater than 65 dB from 0.1 GHz to 6.0 GHz and greater than 60 dB from 6.0 GHz to 12.4 GHz. Reference and test channels track within 0.3-dB amplitude and within 1° phase over any octave band from 0.1 GHz to 8.0 GHz within only a slight degradation at 12.4 GHz. Drift is specified to be within 0.05 dB/°C and 0.1° phase/°C. The primary source of measurement uncertainty is due to test set/connector errors at UHF and microwave frequencies. These uncertainties are quantified as directivity, source match, and frequency tracking errors.

An analytical model for correcting test set/connection errors was implemented based on the model used by Hewlett-Packard for correcting reflectivity measurements on their semiautomated network analyzer system [20]. This model accounts for directivity, frequency tracking, and source match errors [20], [21]. Each of the three types of test set/connection errors is shown schematically in Fig. 5. The term S_{11m} is the measured reflection coefficient, and S_{11a} is the actual reflection coefficient.

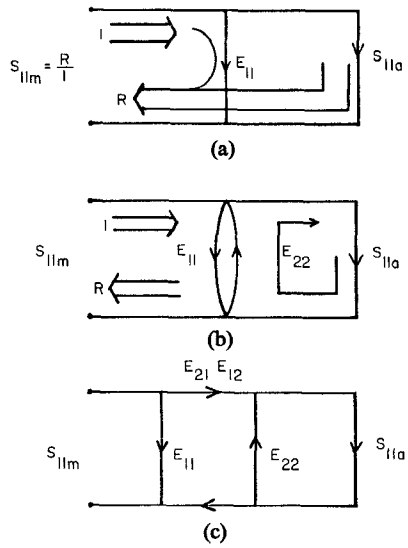

Fig. 5. Error models used for test set/connection errors.

The directivity error E_{11} is due to direct leakage of the incident signal into the reflected signal channel via the reflectometer directional couplers and to further degradation by connectors and adapters. The source match error E_{22} is caused by the rereflection of the reflected signal back to the unknown. $E_{21}E_{12}$, the frequency tracking error, is caused by small variations in gain and phase flatness between the test and reference channels of the analyzer as a function of frequency. These three error terms are determined by calibrating the system using three independent standard terminations, each of whose actual reflection coefficient S_{11a} is known at all frequencies of interest. The measured reflection coefficient S_{11m} expressed as a function of the error terms and the actual reflection coefficient S_{11a} is

$$S_{11m} = E_{11} + \frac{S_{11a}(E_{21}E_{12})}{1 - E_{22}S_{11a}}. \tag{23}$$

The directivity error E_{11} is determined by measuring a sliding matched-load termination. Because no matched load is perfectly matched, multiple load measurements at a number of different path lengths are made. The loci of these points form a circle whose center is the true directivity error vector. The remaining error terms are determined in like manner through the solution of (23). Short-circuit ($S_{11a} = 1 \angle 180°$) and phase compensated open-circuit ($S_{11a} = 1 \angle 0°$) terminations provide the two necessary conditions for determining E_{22} and $E_{21}E_{12}$. Determination of the measurement error terms at each frequency permits one to obtain the actual reflection coefficient as

$$S_{11a} = \frac{S_{11m} - E_{11}}{E_{22}(S_{11m} - E_{11}) + E_{21}E_{12}}. \tag{24}$$

Equation (24) is implemented in the error correction routine which is part of the data processing software on the microcomputer system. Once the measured data are corrected, the remaining data processing software computes the dielectric properties of the test material.

The error correction/calibration model was tested on deionized water in the 2–4-GHz frequency range and compared to standard published data. The water sample impedance data were measured as a complex reflection coefficient, and similar reflection coefficient data were measured for known terminations (short-circuit, open-circuit, and matched loads). A computer algorithm was used to compute the directivity error (E_{11}), the source match error (E_{22}), and the frequency tracking error ($E_{21}E_{12}$) terms in (23). These computed results and the measured water reflection coefficient data (S_{11m}) were then used to compute the actual reflection coefficient (S_{11a}) from (24). The dielectric properties were then computed from the corrected reflection coefficient data. The corrected and uncorrected computed values for the relative dielectric constant and conductivity of water are shown in Fig. 6. In both cases, these data are plotted against an "envelope" which defines the range of normal dielectric property values for water as characterized by standard reference sources [6], [22]–[24] and our previous laboratory measurements [11]. It is noted that accounting for the systemic measurement errors significantly improves the accuracy of the computed results.

IV. Accuracy Studies

The accuracy of the *in vivo* probe measurement system was determined through measurements on a number of standard dielectric materials. Water, methanol, ethylene glycol, and 0.1 molar saline were measured over the 100-MHz–11-GHz frequency range using swept frequency techniques. Figs. 7–10 present graphically the experimentally determined values of relative dielectric constant and loss factor. The worst-case standard-error-of-the-mean (SEM) for each material is noted on the appropriate figure in each case. Data from several reference sources [6], [22]–[24] pertinent to the test materials are also included in the figures for comparison.

Because the reference data available from a single source is rather limited, data from several different reference sources were utilized to establish an adequate base of reference comparison data. An interesting observation is that the variability of data between different reference sources for a specific material measured at the same temperature is often greater than the variability of the data obtained using the *in vivo* measurement probe. Because of the reference source data variability, it is difficult to determine the absolute accuracy of the *in vivo* probe dielectric measurement technique. However, the data measured by the probe are well within the bounds set by the different sources of reference data.

V. Experimental Results

Both *in vivo* and *in vitro* dielectric measurements were performed on several tissue types, which included muscle (canine and rat), kidney (canine), fat (canine), brain (rat), and blood (rat). The results of these measurements and the factors which most affect the accuracy of the *in vivo* probe measurement technique are discussed below.

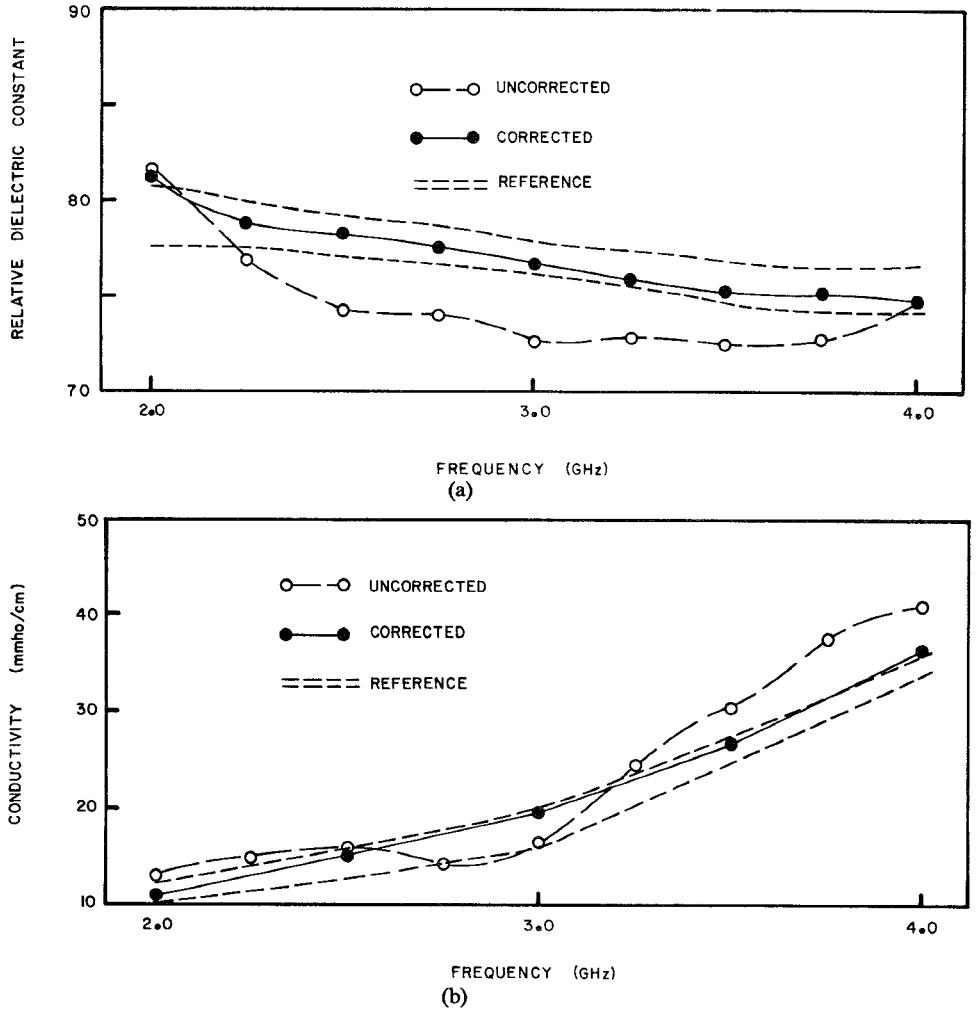

Fig. 6. (a) Relative dielectric constant of deionized water computed from corrected and uncorrected probe measurements compared to the range of dielectric constant data from reference sources. (b) Conductivity of deionized water computed from corrected and uncorrected probe measurements compared to the range of conductivity data from reference sources.

The most significant factors which must be considered while performing *in vivo* tissue dielectric measurements are associated with tissue/probe contact, temperature, and probe positioning. A list of the known factors which affect the accuracy and/or repeatability of *in vivo* probe measurements are the following:

1) tissue dehydration at the measurement area resulting in actual changes in tissue properties;
2) accumulation of dried tissue fluids on the contact surface of the *in vivo* probe which effectively insulate the probe from the tissue;
3) probe contact pressure variations;
4) improper positioning of the probe on the tissue resulting in poor repeatability;
5) changes in tissue temperature resulting in small changes in dielectric properties;
6) actual tissue inhomogeneity in the measurement area.

Each of the above factors constitute a potential error source during the performance of the *in vivo* dielectric measurements, therefore steps to minimize these factors were taken. Tissue dehydration in rat muscle and canine muscle was minimized by covering the measurement area with the skin tissue which had been surgically removed. Although tissue dehydration during *in vivo* measurements performed within the chest cavity of a dog was insignificant, the chest cavity was covered between measurement sets. Dried fluid accumulation at the tip of the measurement probe was prevented by thoroughly cleansing the probe following each measurement sequence. The probe was cleaned by dipping it in metal cleaner and then wiping it thoroughly with methanol. The measured reflection coefficient data were, in some cases, quite sensitive to positioning of the probe on the tissue under study. These measured differences were due to actual tissue property differences at different locations in the same sample which were measurable because of the very small sample volume (0.008 in^3) interrogated by the probe. In order to minimize variations in the measured data, care was taken to position the probe in the exact same measurement location for each measurement repetition. Tissue tempera-

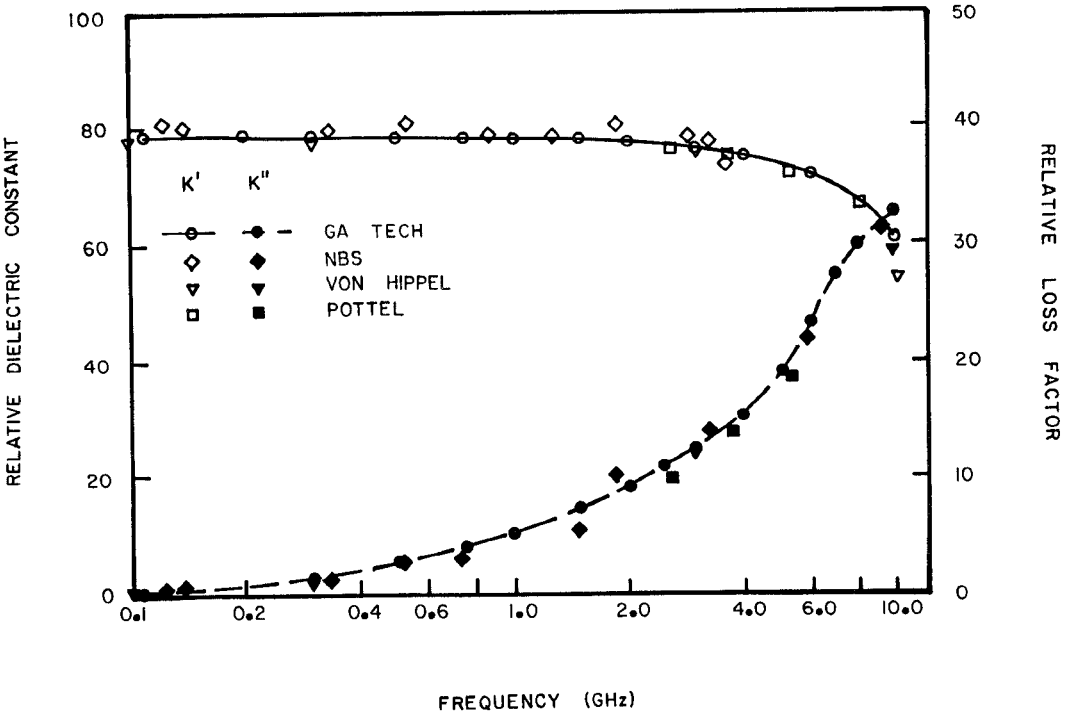

Fig. 7. Experimentally determined relative dielectric constant and relative loss factor of deionized water at 23°C compared to reference data [6], [22]–[24]. Maximum SEM for probe measurements: $K' = \pm 2.75$; $K'' = \pm 2.5$.

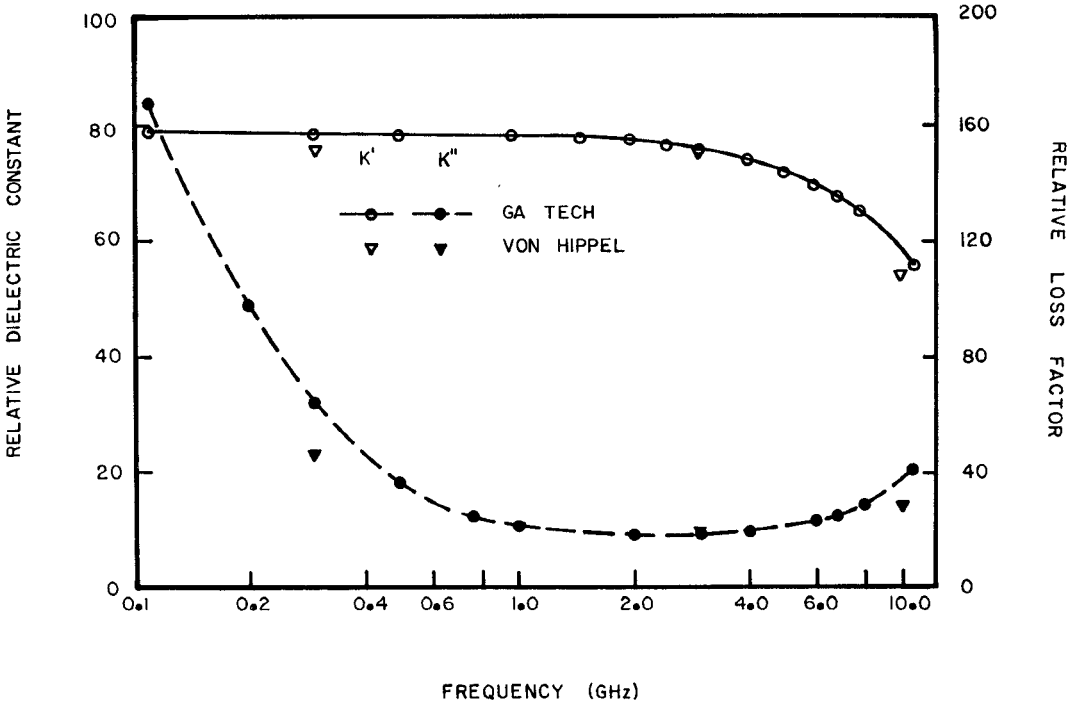

Fig. 8. Experimentally determined relative dielectric constant and relative loss factor of 0.1 molar saline at 23°C compared to reference data [6]. Maximum SEM for probe measurements: $K' = \pm 3.25$; $K'' = 0$.

ture was monitored using a miniature high-resistivity thermistor probe placed on the tissue in an area adjacent to the measurement area, but not close enough to be within the fringing field of the measurement probe. When a decrease in body temperature due to the anesthesia was great enough to be of consequence in the tissue-measurement region, a laboratory lamp was used to heat and maintain the tissue at a constant temperature. Finally, during *in vivo* measurements, a measurement area that contained only one tissue type was selected in order to

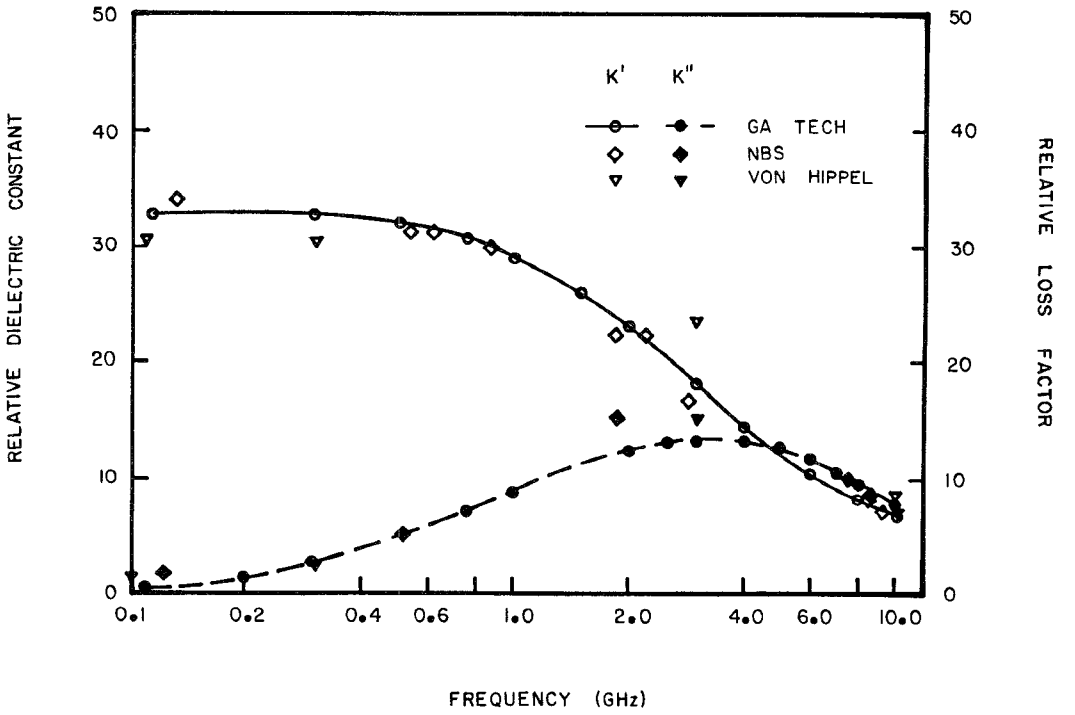

Fig. 9. Experimentally determined relative dielectric constant and relative loss factor of methanol at 23°C compared to reference data [6], [22]. Maximum SEM for probe measurements: $K' = \pm 1.5$; $K'' = \pm 0.9$.

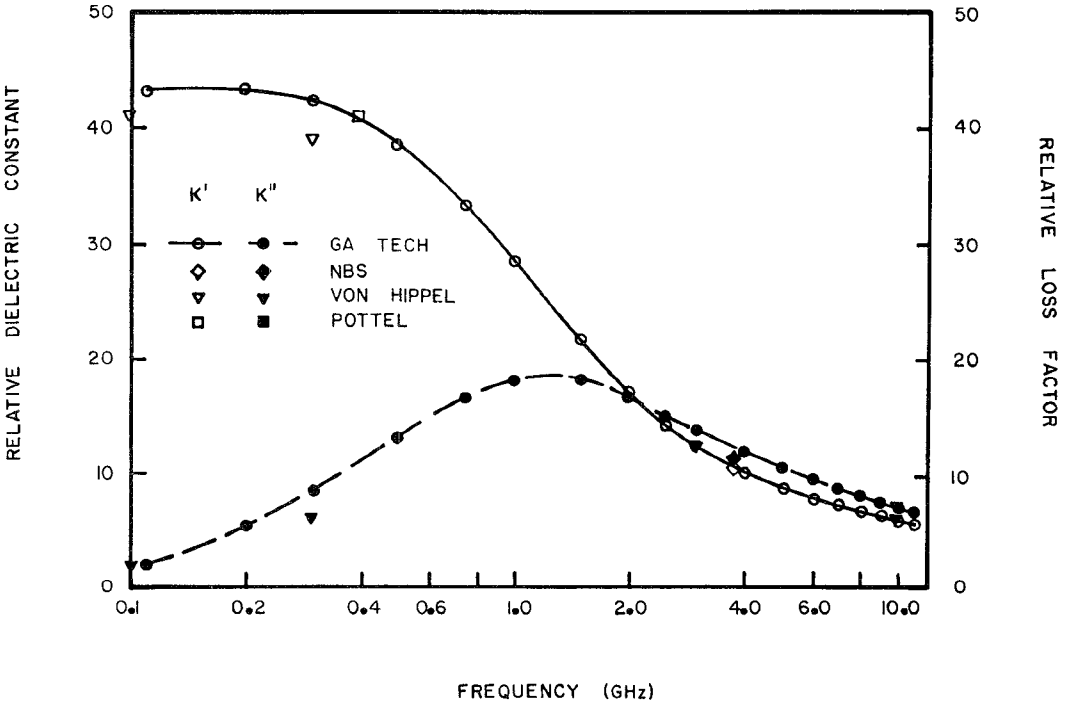

Fig. 10. Experimentally determined relative dielectric constant and relative loss factor of ethylene glycol at 23°C compared to reference data [6], [22]. Maximum SEM for probe measurements: $K' = \pm 1.15$; $K'' = \pm 1.25$.

avoid variations in the measured results due to inhomogeneity of the sample.

The results of the *in vivo* canine and rat tissue measurements are summarized in Figs. 11–15. The relative dielectric constant and conductivity of *in vivo* rat and canine muscle tissue are compared to *in vitro* muscle data from Schwan [25] in Fig. 11. The uncertainty in the measured data is expressed as the SEM and is indicated in the

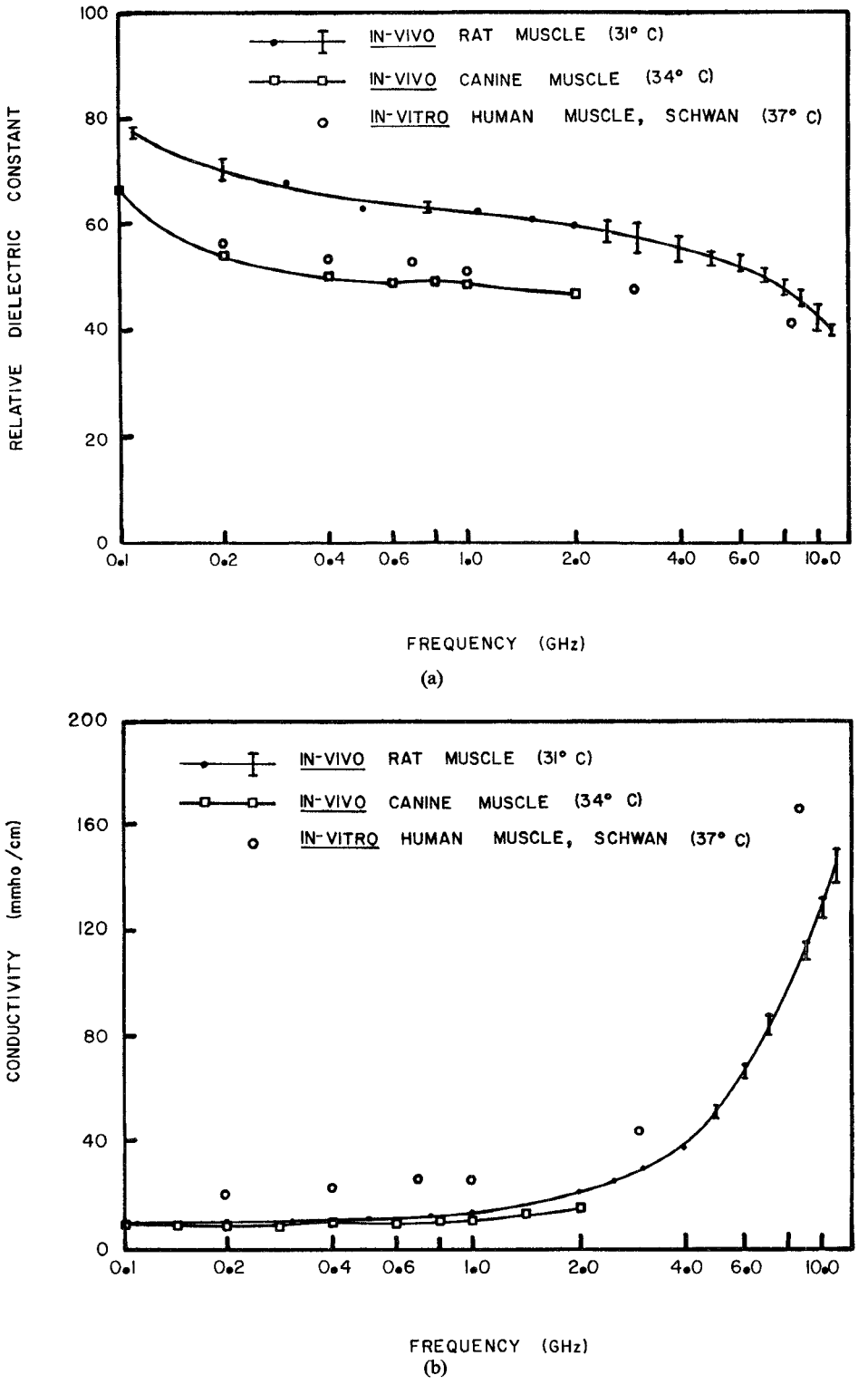

Fig. 11. (a) Experimentally determined relative dielectric constant of *in vivo* rat muscle and canine muscle compared to reference data [25]. (b) Experimentally determined conductivity of *in vivo* rat muscle and canine muscle compared to reference data [25].

figures by the error bars. The difference between the two sets of *in vivo* experimental data are attributed both to differences in the blood perfusion in the different muscle tissues and to the differences in tissue-sample temperature. The differences in the results of the *in vitro* measurements of human autopsy muscle and the *in vivo* measurements of animal muscle could be due to water content, temperature, or actual physiological differences which may exist between living *in situ* and nonliving *in vitro* tissues. Measurement results of *in vivo* and *in vitro* canine kidney cortical tissue are presented in Fig. 12. Again, these results are compared to *in vitro* data from Schwan.

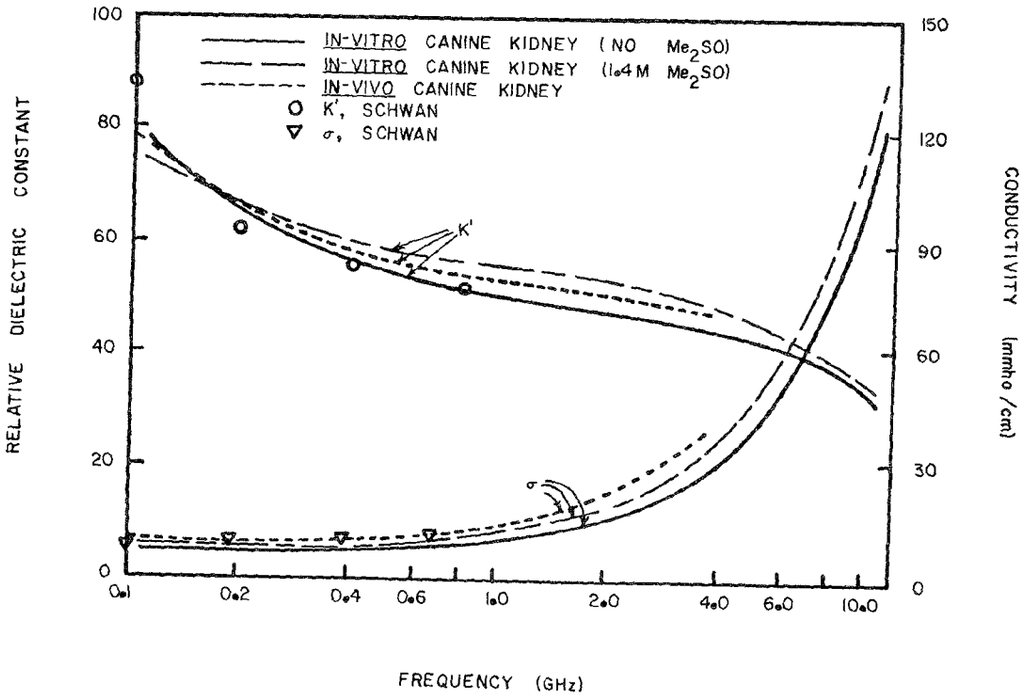

Fig. 12. Experimentally determined relative dielectric constant and conductivity of *in vivo* and *in vitro* canine kidney cortex compared to reference data [25].

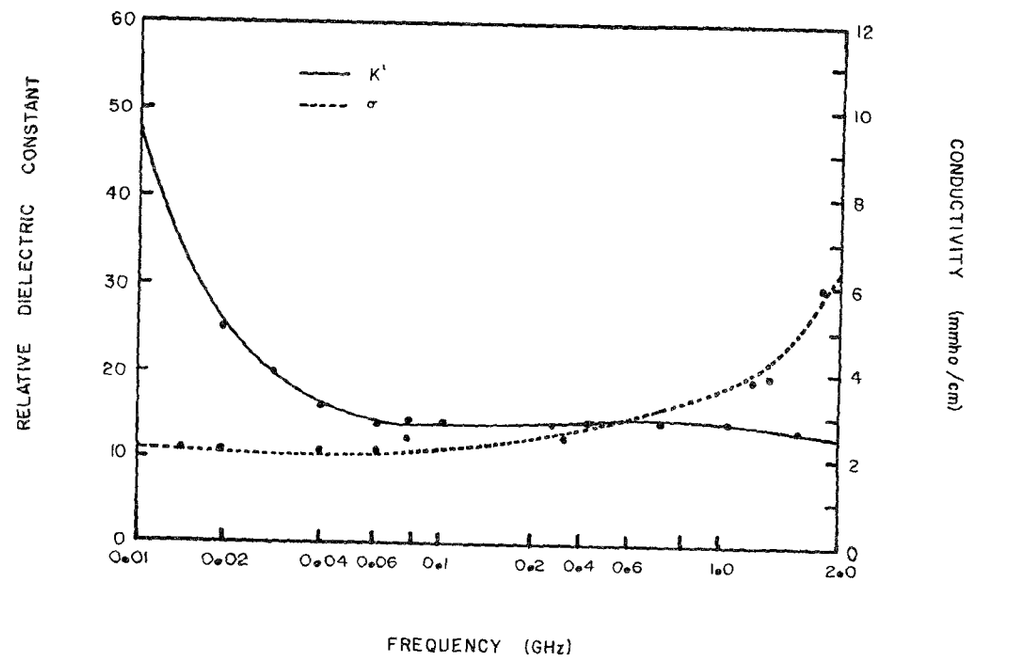

Fig. 13. Experimentally determined relative dielectric constant and conductivity of *in vivo* canine fat tissue at 37°C.

Note that although the *in vitro* data obtained from probe measurements of kidneys without dimethylsulfoxide (Me_2SO) are in close agreement with Schwan's data, the *in vivo* data are different from both sets of *in vitro* data. The results of measurements performed on canine fat, rat brain, and rat blood are shown in Figs. 13–15, respectively. When compared to *in vitro* data [25], [26], the *in vivo* canine fat tissue measurement results (Fig. 13) exhibited relative dielectric constant values a factor of approximately 1.5 to 2 times greater than reported *in vitro* results at frequencies above 100 MHz. These differences in K' are primarily attributed to the possible difference in water content between the *in vivo* and *in vitro* measurement conditions; explicit water content was not reported

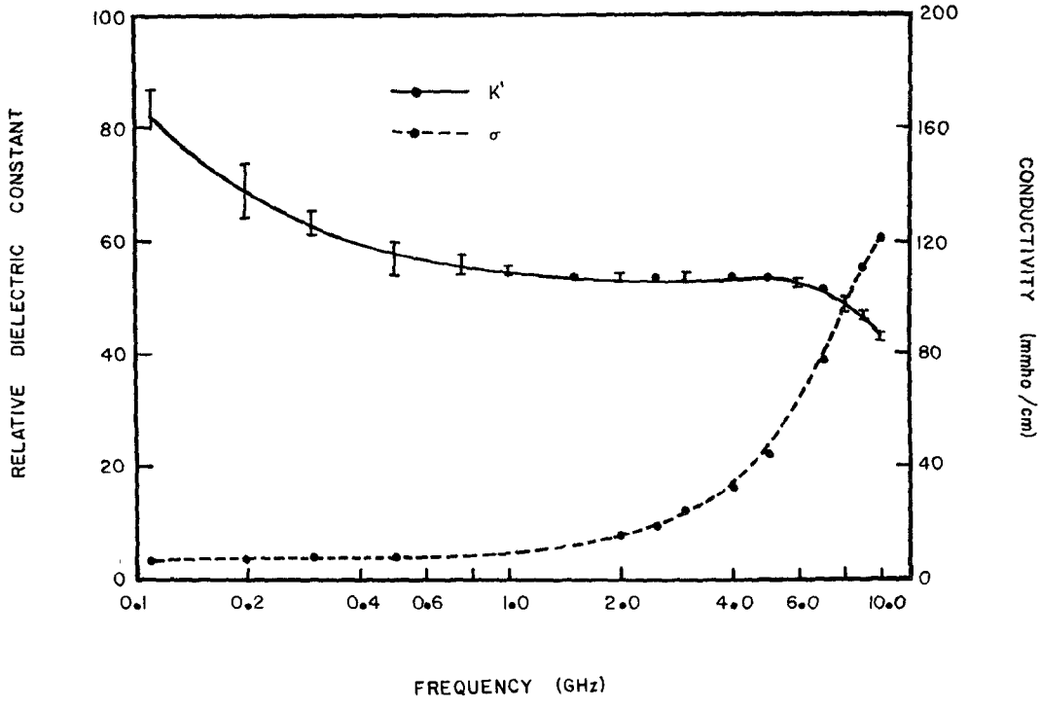

Fig. 14. Experimentally determined relative dielectric constant and conductivity of *in vivo* rat brain at 32°C. Maximum SEM for K' is indicated by error bars and SEM for $K'' = \pm 0.9$.

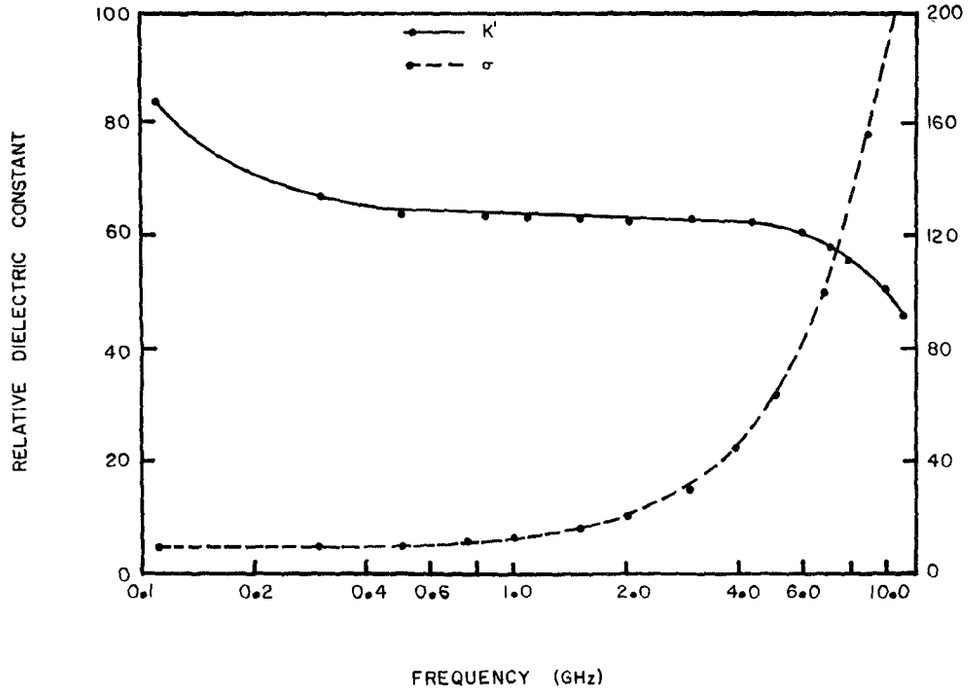

Fig. 15. Experimentally determined relative dielectric constant and conductivity of rat blood at 23°C.

in vitro and no measurement of *in vivo* water content in fat was performed. *In vivo* and reported *in vitro* [25], [26] conductivity values compared very favorably. At all frequencies, the conductivity measured *in vivo* was within the range of reported values nearer the smaller value [26]. The reported *in vitro* values were not included in Fig. 13 because of their wide range.

VI. Summary and Discussion

A system which is capable of performing *in vivo* dielectric property measurements has been developed. Through proper design and use of infinitesimal probes, and by accounting for instrumentation errors through hardware and computer software techniques, swept-frequency

measurements for accurately determining the *in vivo* dielectric property data can be recorded from below 0.1 GHz to above 10 GHz.

A number of *in vivo* probes were fabricated and experimentally evaluated. These probes were infinitesimal monopole measurement probes that were designed both with and without small circular ground planes. Further, the proper designs will permit the accurate measurement of *in vivo* properties for sample volumes as small as 0.008 in^3 (0.13 cm^3) over the 0.1-GHz–10-GHz frequency range. Of the number of probes investigated, the 0.085-in diameter probe was most extensively studied and was found to yield accurate results over the entire frequency range. The probe's measurement accuracy was assessed through measurements of standard liquid dielectric materials including deionized water, methanol, ethylene glycol, and 0.1 molar saline.

The system measurement accuracy was significantly improved at microwave frequencies by incorporating higher precision hardware and systemic error-correction techniques. In order to minimize systemic errors, improved cables were employed. Also, a measurement error correction model was utilized which permits calibration of the system using known terminations (short-circuit, open-circuit, and sliding matched load). The error model thus permits compensation for the remaining systemic measurement errors.

A semiautomated data acquisition/data processing system which permits rapid and accurate data acquisition and computation of the dielectric properties was also developed. This system increased the overall capability of the probe technique by significantly reducing the human involvement in the measurement process and increasing the data processing rate to effectively real time.

In vivo dielectric property measurements were made on a number of tissue types in dogs and rats. The types of tissues measured were canine muscle, canine kidney, canine fat, rat muscle, rat blood, and rat brain. Additionally, measurements addressing the effects of temperature and drugs on dielectric properties were performed. Specifically, the effects of Me_2SO on the dielectric properties of canine kidney tissue were addressed. The *in vivo* dielectric data compiled during the course of these measurements represents, in many cases, the only *in vivo* dielectric information in existence on many of these tissues.

The most significant advantages of the *in vivo* probe-measurement technique over any heretofore available dielectric property measurement techniques are (1) the ability to perform measurements *in vivo* for a wide range of sample volumes, (2) the ability to obtain continuous electrical property data over a wide range of frequencies (0.1 GHz–10 GHz) via swept frequency measurements, and (3) the capability to perform measurement very rapidly. These capabilities could be used to provide data for dosimetry computations for aiding in the establishment of a radiation level with respect to personnel safety and in the planning of treatments for applications of EM hyperthermia to cancer treatment. Further, this measurement technique represents a potentially useful diagnostic tool for detecting changes in certain physiological processes, for differentiating between normal and diseased tissue, or for elucidating deficits due to drugs.

Acknowledgment

The authors wish to thank Dr. F. W. Morthland and Dr. S. Tove at ARO who supported this work, Dr. H. A. Ecker at Scientific-Atlanta, Inc. (formerly at Georgia Tech.), Dr. L. E. Larsen and J. H. Jacobi at the Walter Reed Army Institute of Research, Dr. A. M. Karow, Jr., at the Medical College of Georgia, and J. R. Jones at Georgia Tech., all of whom contributed significantly to this research.

References

[1] *Proc. Int. Symp. on Cancer Therapy by Hypothermia and Radiation*, (Washington, DC), National Cancer Institute, Grant #1 R13 CA 17526, Apr. 28–30, 1975.

[2] H. A. Ecker, E. C. Burdette, and F. L. Cain, "Simultaneous microwave and high frequency thawing of cryogenically preserved canine kidneys," in *1976 IEEE Int. Symp. Electromagn. Compat.*, (Washington, DC), July 1976, pp. 226–230.

[3] H. H. LeVeen, S. Wapnick, V. Piccone, G. Falk, and N. Ahmed, "Tumor eradication by radiofrequency therapy: Response in 21 patients," *JAMA*, vol. 235, no. 20, pp. 2198–2200, May 17, 1975.

[4] E. C. Burdette, and A. M. Karow, "Kidney model for study of electromagnetic thawing," *Cryobiology-Int. J. Low Temperature Bio. and Medicine*, vol. 15, no. 2, pp. 142–151, Apr. 1978.

[5] S. M. Michaelson, "Human exposure to nonionizing radiant energy—potential hazards and safety standards," *Proc. IEEE*, vol. 60, pp. 387–421, Apr. 1972.

[6] A. R. Von Hippel, *Dielectric Materials and Applications*. Cambridge, MA: M. I. T. Press, 1954, pp. 36–40, 301–425.

[7] W. S. Spector, *Handbook of Biological Data*, W. B. Saunders, 1956, p. 291.

[8] E. C. Burdette, and J. Seals, "A technique for determining the electrical properties of living tissues at VHF through microwave frequencies," in *Proc. 1977 IEEE Region Three Conf. and Exhibit*, Apr. 1977, pp. 120–123.

[9] E. C. Burdette, J. Seals, J. C. Toler, and F. L. Cain, "Preliminary in-vivo probe measurements of electrical properties of tumors in mice," in *Dig. 1977 IEEE MTT-S Int. Microwave Symp.*, (San Diego, CA), pp. 344–348, June 1977.

[10] H. A. Ecker, E. C. Burdette, F. L. Cain, and J. Seals, "In-vivo determination of energy absorption in biological tissue," U.S. Army Research Office, Annual Tech. Rep., Project A-1755, Grant DAAG29-75-G-0182, July 1976.

[11] F. L. Cain, E. C. Burdette, and J. Seals, "In-vivo determination of energy absorption in biological tissue," U.S. Army Research Office, Annual Tech. Rep., Project A-1755, Grant DAAG29-75-G-0182, July 1977.

[12] E. C. Burdette, F. L. Cain, and J. Seals, "In-vivo determination of energy absorption in biological tissue," U. S. Army Research Office, Final Tech. Rep., Project A-1755, Grant DAAG29-75-G-0182, Jan. 1979.

[13] G. A. Deschamps, "Impedance of an antenna in a conducting medium," *IRE Trans. Antennas Propagat.*, Sept. 1962, pp. 648–650.

[14] C. T. Tai, "Characteristics of Linear Antenna Elements," in *Antenna Engineering Handbook*, H. Jasik, ed. New York: McGraw-Hill, 1961, ch. 3, p. 2.

[15] R. L. Magin, and C. P. Burns, "Determination of biological tissue dielectric constant and resistivity from in-vivo impedance measurements," in *Region Three Conf. IEEE*, Apr. 1972.

[16] J. H. Richmond, "A reaction theorem and its application to antenna impedance calculations," *IRE Trans. Antennas Propagat.*, Nov. 1961, pp. 515–520.

[17] R. F. Harrington, *Time Harmonic Electromagnetic Fields*. New York: McGraw-Hill, 1961, pp. 110–113.
[18] E. C. Jordon, and K. G. Balmain, *Electromagnetic Waves and Radiating Systems*. Englewood Cliffs, NJ: Prentice-Hall, 1968, pp. 323–326.
[19] G. H. Brown, and O. M. Woodward, Jr., "Experimentally determined impedance characteristics of cylindrical antennas," *Proc. IRE*, pp. 257—262, Apr. 1945.
[20] "Semi-automated measurements using the 8410B microwave network analyzer and the 9825A desk-top computer," Hewlett-Packard Application Note 221, Mar. 1977.
[21] E. F. da Silva, and M. K. McPhun, "Calibration techniques for one port measurement," *Microwave J.*, pp. 97–100, June 1978.
[22] F. Buckley, and A. A. Maryott, "Tables of dielectric dispersion data for pure liquids and dilute solutions," Nat. Bur. Stand. Circular 589, Nov. 1958.
[23] H. F. Cook, "A Comparison of the dielectric behavior of pure water and human blood at microwave frequencies," *Brit. J. of Appl. Phys.*, vol. 3, pp. 249–255, Aug. 1952.
[24] J. B. Hasted, *Water: A Comprehensive Treatise (The Physics of Physical Chemistry of Water)*, vol. 2, F. Franks, Ed. New York: Plenum, 1972, pp. 255–305.
[25] H. P. Schwan, "Electrical Properties of Tissues and Cells," in *Advances in Biological and Medical Physics*, vol. V, J. H. Lawrence and C. A. Tobias, Eds. New York: Academic, 1957, pp. 147–209.
[26] C. C. Johnson, and A. W. Guy, "Nonionizing electromagnetic wave effects in biological materials and systems," *Proc. IEEE*, vol. 60, pp. 694–695, June 1972.